

# Rapid adaptation of harmful cyanobacteria to rising CO<sub>2</sub>

Giovanni Sandrini<sup>a,1</sup>, Xing Ji<sup>a,1</sup>, Jolanda M. H. Verspagen<sup>a</sup>, Robert P. Tann<sup>a</sup>, Pieter C. Slot<sup>a</sup>, Veerle M. Luimstra<sup>a,b</sup>, J. Merijn Schuurmans<sup>a,c</sup>, Hans C. P. Matthijs<sup>a,2</sup>, and Jef Huisman<sup>a,3</sup>

<sup>a</sup>Department of Aquatic Microbiology, Institute for Biodiversity and Ecosystem Dynamics, University of Amsterdam, 1090 GE Amsterdam, The Netherlands; <sup>b</sup>Wetsus, European Centre of Excellence for Sustainable Water Technology, 8900 CC Leeuwarden, The Netherlands; and <sup>c</sup>Department of Aquatic Ecology, Netherlands Institute of Ecology, 6700 AB Wageningen, The Netherlands

Edited by Paul G. Falkowski, Rutgers, The State University of New Jersey, New Brunswick, NJ, and approved June 10, 2016 (received for review February 12, 2016)

Rising atmospheric CO<sub>2</sub> concentrations are likely to affect many ecosystems worldwide. However, to what extent elevated CO<sub>2</sub> will induce evolutionary changes in photosynthetic organisms is still a major open question. Here, we show rapid microevolutionary adaptation of a harmful cyanobacterium to changes in inorganic carbon (C<sub>i</sub>) availability. We studied the cyanobacterium *Microcystis*, a notorious genus that can develop toxic cyanobacterial blooms in many eutrophic lakes and reservoirs worldwide. *Microcystis* displays genetic variation in the C<sub>i</sub> uptake systems BicA and SbtA, where BicA has a low affinity for bicarbonate but high flux rate, and SbtA has a high affinity but low flux rate. Our laboratory competition experiments show that *bicA* + *sbtA* genotypes were favored by natural selection at low CO<sub>2</sub> levels, but were partially replaced by the *bicA* genotype at elevated CO<sub>2</sub>. Similarly, in a eutrophic lake, *bicA* + *sbtA* strains were dominant when C<sub>i</sub> concentrations were depleted during a dense cyanobacterial bloom, but were replaced by strains with only the high-flux *bicA* gene when C<sub>i</sub> concentrations increased later in the season. Hence, our results provide both laboratory and field evidence that increasing carbon concentrations induce rapid adaptive changes in the genotype composition of harmful cyanobacterial blooms.

climate change | harmful algal blooms | *Microcystis aeruginosa* | microevolution | natural selection

Atmospheric CO<sub>2</sub> concentrations are predicted to double during this century (1, 2). Species may adapt to elevated CO<sub>2</sub> by the sorting of existing genetic variation and the establishment of new beneficial mutations. These evolutionary processes can alter the physiological and ecological response of photosynthetic species to future CO<sub>2</sub> levels (3). Several recent laboratory studies have investigated the potential for evolutionary changes in response to rising CO<sub>2</sub> concentrations (4–9). For example, selection experiments with the green alga *Chlamydomonas reinhardtii* revealed that some cell lines grown at elevated CO<sub>2</sub> levels for 1,000 generations had obtained a reduced growth rate at ambient CO<sub>2</sub>, presumably because mutations reduced the effectiveness of CO<sub>2</sub> acquisition (4, 5). Other laboratory studies argue that elevated atmospheric CO<sub>2</sub> fails to evoke specific evolutionary adaptation in phytoplankton species (7). Thus far, however, the specific genetic and molecular adaptations to rising CO<sub>2</sub> favored by natural selection are not well understood. Furthermore, adaptation to changing CO<sub>2</sub> conditions has rarely been investigated within complex species assemblages (9) and, to our knowledge, has never been reported from natural waters.

Cyanobacteria produce dense and often toxic blooms in many eutrophic lakes worldwide (10–12), and are likely to benefit from eutrophication and global warming (10, 13–15). Dense cyanobacterial blooms can deplete the dissolved CO<sub>2</sub> [CO<sub>2</sub>(aq)] concentration (16–18), which provides an opportunity to study adaptation to changes in carbon availability. Cyanobacteria are often thought to be superior competitors when CO<sub>2</sub>(aq) concentrations are depleted, because they use a very effective CO<sub>2</sub>-concentrating mechanism (CCM) (19, 20). The cyanobacterial CCM is based on the uptake of CO<sub>2</sub> and bicarbonate, and subsequent accumulation of inorganic

carbon (C<sub>i</sub>) in specialized compartments, called carboxysomes, for CO<sub>2</sub> fixation by the enzyme RuBisCO (21). Five C<sub>i</sub> uptake systems are known in cyanobacteria. Two CO<sub>2</sub> uptake systems and the ATP-dependent bicarbonate transporter BCT1 are present in most freshwater cyanobacteria (15, 21–23). Two other bicarbonate uptake systems, BicA and SbtA, are less widespread. Both are sodium-dependent symporters, but BicA has a low affinity for bicarbonate and high flux rate, whereas SbtA has a high affinity and low flux rate (21, 24). Affinity refers here to the effectiveness of bicarbonate uptake at low bicarbonate concentrations, whereas the flux rate refers to the bicarbonate uptake rate at high bicarbonate concentrations.

We recently compared CCM gene sequences of 20 strains of *Microcystis* (23), a ubiquitous cyanobacterium that can produce a potent family of hepatotoxins known as microcystins (25). The strains were very similar in their CCM gene composition, but interestingly some strains lacked the high-flux bicarbonate uptake gene *bicA*, whereas others lacked the high-affinity bicarbonate uptake gene *sbtA*. Hence, three different C<sub>i</sub> uptake genotypes can be distinguished (23): *sbtA* strains (with *sbtA* but no or incomplete *bicA*), *bicA* strains (with *bicA* but no *sbtA*), and *bicA* + *sbtA* strains (Fig. 1). The three genotypes produce different phenotypes. Laboratory experiments showed that the growth rate of the *sbtA* genotype is reduced at high C<sub>i</sub> levels, the *bicA* genotype has reduced growth at low C<sub>i</sub> levels, whereas the *bicA* + *sbtA* genotype maintains a constant growth rate across a wide range of C<sub>i</sub> levels (23). Little is known, however, about the occurrence of these three C<sub>i</sub> uptake genotypes in lakes, and how

## Significance

Cyanobacterial blooms pose a major threat to the water quality of many eutrophic lakes and reservoirs. Cyanobacteria are thought to be very effective competitors when CO<sub>2</sub> levels are depleted during dense blooms. Their response to elevated CO<sub>2</sub> is less understood, however. We study competition among cyanobacteria, and find both laboratory and field evidence for natural selection of strains with different carbon uptake systems at different CO<sub>2</sub> levels. Our results demonstrate that changes in inorganic carbon availability act as an important selective factor in cyanobacterial communities and suggest that future harmful cyanobacterial blooms will have a genotype composition that differs from contemporary blooms and will be tuned to the high-CO<sub>2</sub> conditions.

Author contributions: G.S., X.J., J.M.H.V., H.C.P.M., and J.H. designed research; G.S., X.J., J.M.H.V., R.P.T., P.C.S., V.M.L., J.M.S., and H.C.P.M. performed research; G.S. contributed new reagents/analytic tools; G.S., X.J., J.M.H.V., H.C.P.M., and J.H. analyzed data; and G.S., X.J., H.C.P.M., and J.H. wrote the paper.

The authors declare no conflict of interest.

This article is a PNAS Direct Submission.

<sup>1</sup>G.S. and X.J. contributed equally to this work.

<sup>2</sup>Deceased April 17, 2016.

<sup>3</sup>To whom correspondence should be addressed. Email: j.huisman@uva.nl.

This article contains supporting information online at [www.pnas.org/lookup/suppl/doi:10.1073/pnas.1602435113/-DCSupplemental](http://www.pnas.org/lookup/suppl/doi:10.1073/pnas.1602435113/-DCSupplemental).

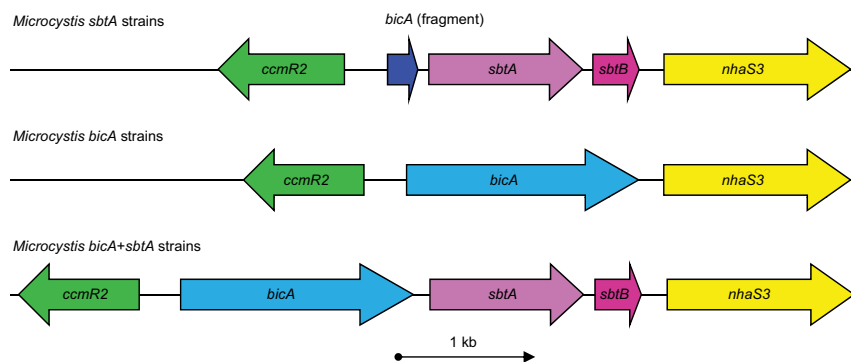


**Fig. 1.** The three  $C_i$  uptake genotypes of *Microcystis*. The variable genomic regions contain the transcriptional regulator gene *ccmR2*, the sodium-dependent bicarbonate uptake genes *bicA* and *sbtA*, a posttranslational regulator gene of SbtA known as *sbtB*, and the sodium/proton antiporter gene *nhaS3*.

their relative frequencies may change in response to increasing  $C_i$  concentrations. Here, we test the potential for adaptive microevolution of *Microcystis* in response to elevated  $CO_2$ , by investigating changes in the relative frequencies of the different  $C_i$  uptake genotypes in laboratory competition experiments and a lake study.

## Results

**Competition Experiments.** We ran competition experiments in three chemostats at low  $CO_2$  (100 ppm) and three chemostats at high  $CO_2$  (1,000 ppm) levels. Each chemostat was inoculated with five *Microcystis* strains, including two *sbtA* strains (CCAP 1450/10 and HUB 5-2-4), one *bicA* strain (PCC 7806) and two *bicA* + *sbtA* strains (PCC 7005 and PCC 7941) (*SI Appendix, Table S1*). Four strains produced the hepatotoxin microcystin, whereas PCC 7005 was the only nontoxic strain. In the low  $CO_2$  chemostats, the total *Microcystis* biomass increased until a steady state was reached, at which the  $CO_2(aq)$  and bicarbonate concentration were depleted to  $1.5 \times 10^{-4} \mu\text{mol}\cdot\text{L}^{-1}$  and  $15 \mu\text{mol}\cdot\text{L}^{-1}$ , respectively, and pH increased to 11.2 (Fig. 2 *A* and *C*). The high  $CO_2$  chemostats produced a 2.5-fold higher *Microcystis* biomass, with much higher steady-state  $CO_2(aq)$  and bicarbonate concentrations of  $10 \mu\text{mol}\cdot\text{L}^{-1}$  and  $2,700 \mu\text{mol}\cdot\text{L}^{-1}$ , respectively, and a lower pH of 8.8 (Fig. 2 *B* and *D*).

In the low  $CO_2$  chemostats, the toxic *bicA* + *sbtA* strain PCC 7941 competitively replaced the two *sbtA* strains, the *bicA* strain, and the nontoxic *bicA* + *sbtA* strain, and comprised  $\sim 90\%$  of the total *Microcystis* population at steady state (Fig. 2*E*). In contrast, in the high  $CO_2$  chemostats, the nontoxic *bicA* + *sbtA* strain PCC 7005 coexisted with the toxic *bicA* strain PCC 7806, with relative abundances of  $\sim 60\%$  and  $\sim 30\%$ , respectively, at steady state (Fig. 2*F*). Selection coefficients, calculated from the replacement rates of the strains and their generation times, ranged from 0.16 to 0.62 in the low  $CO_2$  chemostats and from 0.08 to 0.20 in the high  $CO_2$  chemostats (*SI Appendix, Fig. S1* and *Table S2*).

**Lake Study.** Our field study was carried out in Lake Kennemermeer, a slightly brackish coastal dune lake in The Netherlands, in summer and autumn of 2013 (Fig. 3*A*). Water temperature was  $20\text{--}23^\circ\text{C}$  in summer, and then gradually declined to  $11^\circ\text{C}$  in early autumn (*SI Appendix, Fig. S2*). The lake contained high phytoplankton abundances, with particularly dense blooms in weeks 26–28 and week 36 (Fig. 3*B*). The phytoplankton community consisted largely of cyanobacteria ( $>95\%$  of the total biovolume), including Pseudanabaenaceae, small Chroococcales, *Anabaenopsis hungarica* and *Microcystis* spp. The *Microcystis* population was dominated by potentially toxic genotypes containing the microcystin synthetase gene *mcyB* (*SI Appendix, Fig. S2*). Concentrations of *Microcystis* and the two dominant microcystin types, MC-LR and MC-RR, peaked in week 34 (Fig. 3*C*). The MC-LR concentration (up to  $23.2 \mu\text{g}\cdot\text{L}^{-1}$ ) exceeded the provisional

guideline for safe drinking water ( $1 \mu\text{g}\cdot\text{L}^{-1}$ ) of the World Health Organization and common guidelines for recreational waters (26), justifying closure of the lake for recreation.

In summer,  $CO_2(aq)$  concentrations in the lake were reduced below  $3.5 \mu\text{mol}\cdot\text{L}^{-1}$  and were strongly depleted to  $<0.4 \mu\text{mol}\cdot\text{L}^{-1}$  in weeks 28–30 and week 36 (Fig. 3*D*). When phytoplankton abundance decreased in autumn, the  $CO_2(aq)$  concentration increased to  $\sim 15 \mu\text{mol}\cdot\text{L}^{-1}$ , equilibrating with the atmospheric  $pCO_2$  levels (390 ppm).  $CO_2$  depletion during the summer bloom led to a strong increase in pH, with values up to  $\sim 10$  during the two peaks in phytoplankton abundance (Fig. 3*B*) (Pearson correlation of pH vs.  $\log CO_2$ :  $r = -0.98$ ,  $n = 10$ ,  $P < 0.001$ ). At pH between 8 and 10, bicarbonate is the dominant  $C_i$  species. Bicarbonate concentrations showed similar temporal dynamics as the  $CO_2(aq)$  concentration, with relatively low bicarbonate concentrations during the summer blooms and higher concentrations in autumn (Fig. 3*D*) [Pearson correlation of  $CO_2(aq)$  vs. bicarbonate:  $r = 0.90$ ,  $n = 10$ ,  $P < 0.001$ ]. The sodium concentration in the lake (measured in week 29) was  $12.7 \pm 0.4 \text{ mmol}\cdot\text{L}^{-1}$ , which allows maximum or near-maximum activity of the sodium-dependent bicarbonate transporters BicA and SbtA, because both transporters have half-saturation constants of  $1\text{--}2 \text{ mmol}\cdot\text{L}^{-1}$  sodium (24, 27).

All three  $C_i$  uptake genotypes of *Microcystis* were present in the lake (Fig. 1 and *SI Appendix, Tables S3* and *S4*), but their relative abundances changed during the study period (Fig. 4*A*). The *sbtA* strains represented  $\sim 20\%$  of the *Microcystis* population during the entire season (Fig. 4*B*). The *bicA* + *sbtA* strains dominated the *Microcystis* population in weeks 24–32, especially during the strong  $CO_2$  depletion in weeks 28–29, but were largely replaced by *bicA* strains in late summer and autumn when  $C_i$  concentrations in the lake increased. Relative abundances of the *bicA* + *sbtA* strains were negatively correlated with the bicarbonate concentration (Fig. 4*C*) (Pearson correlation:  $r = -0.84$ ,  $n = 10$ ,  $P < 0.01$ ), whereas those of the *bicA* strains were positively correlated with bicarbonate (Fig. 4*D*) (Pearson correlation:  $r = 0.91$ ,  $n = 10$ ,  $P < 0.001$ ). Replacement of *bicA* + *sbtA* strains by *bicA* strains occurred in  $\sim 2$  months. With a generation time of 1.5–5.2 d (28), this corresponds to 12–42 generations and a selection coefficient of 0.06–0.19 per generation, which is comparable to the selection coefficients in the chemostats (*SI Appendix, Fig. S3* and *Table S2*).

## Discussion

Our laboratory competition experiments and lake study show qualitatively similar changes in strain composition. In both systems, the *Microcystis* population was dominated by *bicA* + *sbtA* strains at low  $C_i$  levels that were (partly) replaced by *bicA* strains at high  $C_i$  levels (Figs. 2 and 4). Previous studies have shown that the high-affinity but low-flux bicarbonate uptake system SbtA is more effective at low bicarbonate concentrations, whereas the

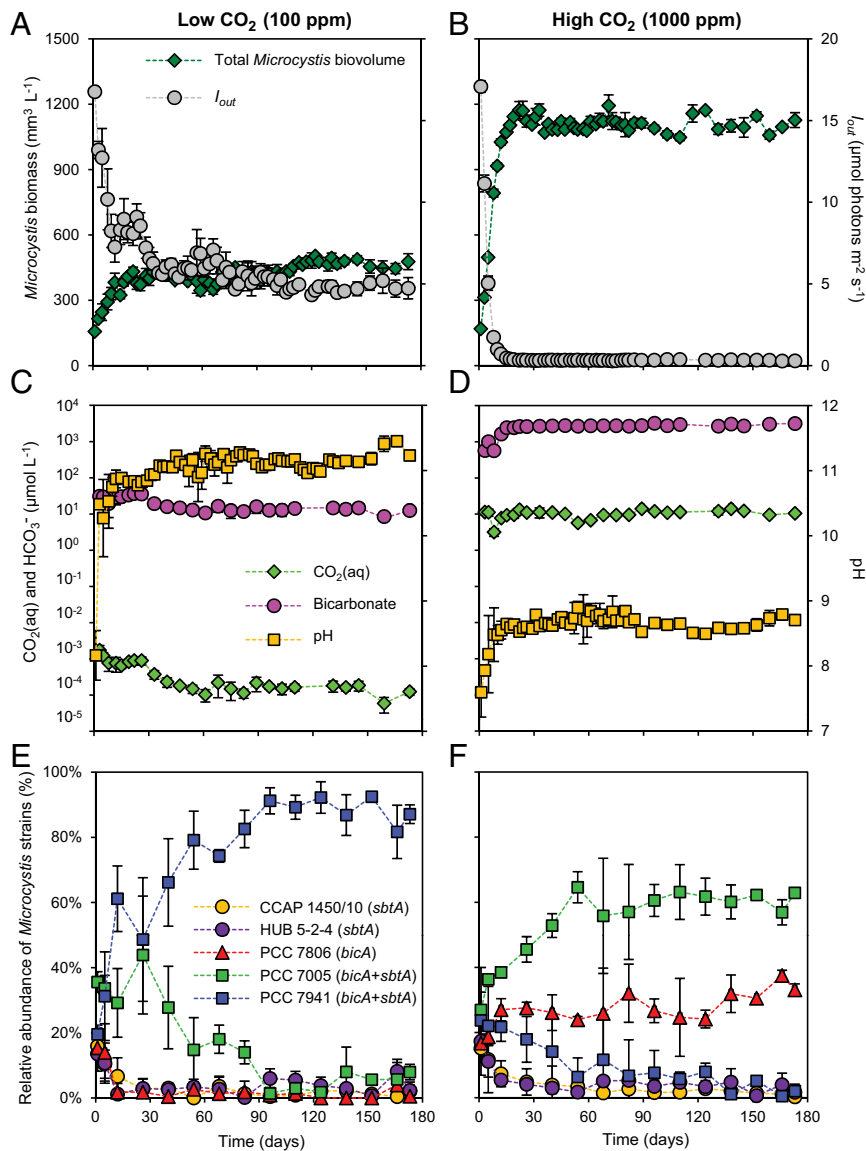


**Fig. 2.** Laboratory competition experiments with five *Microcystis* strains at low and high CO<sub>2</sub> levels. (*Left*) Low CO<sub>2</sub> chemostats. (*Right*) High CO<sub>2</sub> chemostats. (*A and B*) *Microcystis* biomass (expressed as biovolume) and the light intensity  $I_{out}$  transmitted through the chemostats. (*C and D*) Concentrations of dissolved CO<sub>2</sub> [CO<sub>2</sub>(aq)] and bicarbonate, and pH. (*E and F*) Relative abundances of the five *Microcystis* strains. The data points show the mean values ( $\pm$ SD) of three replicated chemostat experiments.

low-affinity but high-flux enzyme BicA is more effective at high bicarbonate concentrations (23, 24). Hence, the trade-off between affinity and flux rate offers a likely explanation for the observed shift in strain composition. In particular, with increasing CO<sub>2</sub> and bicarbonate concentrations, high-affinity bicarbonate uptake systems are no longer needed. We note that in *bicA + sbtA* strains of *Microcystis*, *bicA* and *sbtA* are located on the same operon and hence are cotranscribed (23). Superfluous transcription of *sbtA* or posttranscriptional down-regulation of the SbtA enzyme, for example by SbtB (27), will be costly when SbtA cannot be efficiently used, which will disfavor *bicA + sbtA* strains at high bicarbonate concentrations. Our results thus provide both laboratory and field evidence demonstrating that *bicA* strains; that is, strains with low-affinity but high-flux bicarbonate uptake systems, have a selective advantage at high C<sub>i</sub> availability.

In addition to bicarbonate uptake systems, cyanobacteria also deploy two intracellular CO<sub>2</sub> “uptake” systems, which convert CO<sub>2</sub> passively diffusing into the cell into bicarbonate (21, 29, 30).

In all *Microcystis* strains investigated so far, both CO<sub>2</sub> uptake systems were present (23) and the genes encoding these two CO<sub>2</sub> uptake systems were constitutively expressed (31–33). A possible explanation might be that the sustained activity of both intracellular CO<sub>2</sub> uptake systems helps to maintain a low CO<sub>2</sub>(aq) concentration in the cytoplasm, thus maximizing the diffusive influx of CO<sub>2</sub>. Bloom-forming cyanobacteria like *Microcystis* usually occur in mildly to highly alkaline waters (pH > 7.5), where bicarbonate concentrations are much higher than the CO<sub>2</sub>(aq) concentration (Fig. 3D). Laboratory studies have shown that the high-affinity bicarbonate uptake system BCT ceases its activity, whereas the BicA enzyme remains active at elevated CO<sub>2</sub> levels (31, 32), and that bicarbonate still accounts for most of the C<sub>i</sub> uptake even at elevated CO<sub>2</sub> levels (34–36). Hence, in alkaline waters, adaptation of the bicarbonate uptake systems to changes in C<sub>i</sub> availability is indeed likely to have major fitness consequences.

Quantitatively, *bicA* strains responded more strongly to increasing C<sub>i</sub> concentrations in the lake than in the chemostat

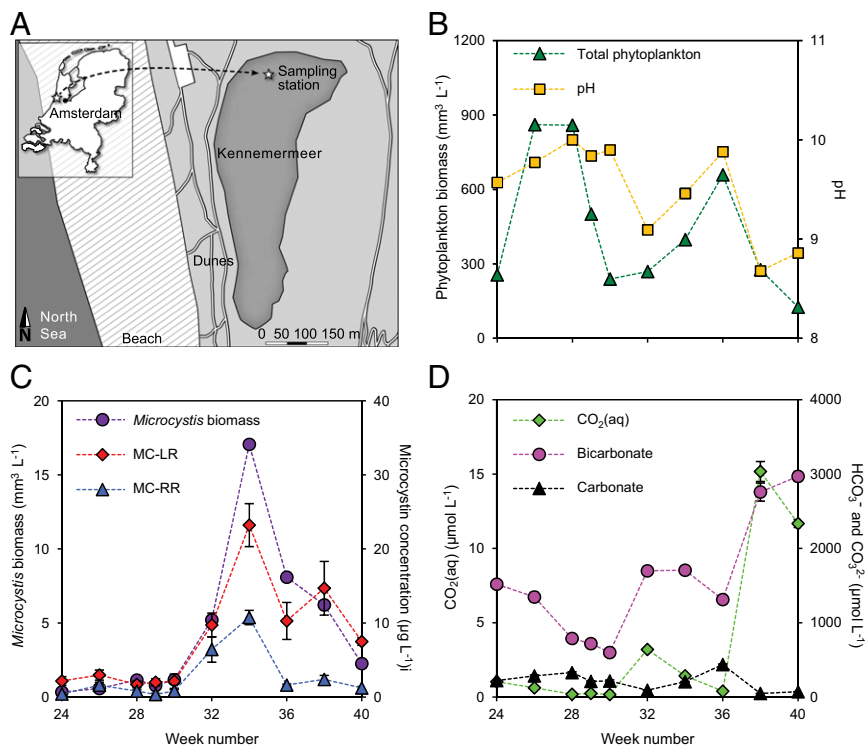


**Fig. 3.** Phytoplankton biomass and inorganic carbon speciation in Lake Kennemermeer. (A) Map of Lake Kennemermeer with the sampling station. (B) Total phytoplankton biomass (expressed as biovolume) and pH. (C) *Microcystis* biomass (expressed as biovolume) and concentrations of the two most abundant microcystin variants (MC-LR and MC-RR). (D) Concentrations of  $\text{CO}_2(\text{aq})$ , bicarbonate, and carbonate. Data points represent the mean ( $\pm$ SD) of three replicate measurements; error bars that are not visible do not exceed the size of the symbols.

experiments, whereas *sbtA* strains persisted in the lake but were competitively excluded from the chemostats. These dissimilarities might be attributed to differences in environmental conditions between lakes and laboratory experiments. For example, the chemostat experiments used continuous illumination, whereas *Microcystis* in Lake Kennemermeer experienced large daily fluctuations in both light conditions and inorganic carbon concentrations, which induced diel variation in expression of the bicarbonate uptake genes and several other CCM genes (33). Furthermore, the chemostats applied homogeneous mixing to single-celled *Microcystis* populations, whereas *Microcystis* often develops multicellular colonies migrating vertically in stagnant lakes (37). *Microcystis* is also known to survive prolonged burial in lake sediments, after which it can be resuspended in the water column (38). Both spatiotemporal heterogeneity and reseeding from the sediments tend to promote diversity, and may explain the observed co-occurrence of all three  $\text{C}_i$  uptake genotypes in the lake.

Some of our results may also be due to further variation among *Microcystis* strains other than their  $\text{C}_i$  uptake genes (39, 40). For instance, the strains in our selection experiments differed in the production of microcystin. In addition to its toxicity to humans and mammals, microcystin can also bind to cyanobacterial proteins such as the RuBisCO enzyme to offer protection against oxidative stress (41). Carbon-limited conditions are likely to induce more oxidative stress than elevated  $\text{CO}_2$  concentrations, which may explain why the microcystin-producing *bicA* + *sbtA* strain PCC 7941 performed better at 100 ppm  $\text{CO}_2$ , whereas the nonmicrocystin-producing *bicA* + *sbtA* strain PCC 7005 performed better at 1,000 ppm (Fig. 2). Our lake study, however, did not show a relation between the relative abundance of microcystin-producing strains and the  $\text{C}_i$  concentrations (SI Appendix, Fig. S2C), indicating that selection among the different  $\text{C}_i$  uptake genotypes played a much

larger role in the adaptation to changing  $\text{C}_i$  concentrations than genetic variation in microcystin production.

Our results add to the growing literature showing that plankton species are capable of rapid evolutionary adaptation to changing conditions; for example, in response to rising  $\text{CO}_2$  levels (6, 8, 9), increasing temperature (42, 43), and changes in predation pressure (44, 45). A key advance of the present work is that the adaptive changes could be linked to specific genetic and molecular traits, which enabled monitoring of natural selection not only in confined laboratory experiments but also in lakes. In our study, and several previous studies (6, 42–45), the adaptive changes are most likely caused by sorting of existing genetic variation rather than by de novo mutations. This implies that at the time scale of cyanobacterial bloom development, the traits (in this case, the  $\text{C}_i$  uptake kinetics) of cyanobacterial species may change due to a reshuffling of the relative abundances of different genotypes within the species. Hence, predictions of harmful algal bloom development cannot be based on the assumption that species traits remain constant. Instead, an ecoevolutionary approach will be required (46–48), in which traits evolve in response to changes in environmental conditions that, in the case of  $\text{CO}_2$  depletion, are at least partly induced by the phytoplankton blooms themselves.

In conclusion, our study shows that changes in  $\text{C}_i$  availability act as an important selective factor in cyanobacterial communities. Some strains perform better at low  $\text{C}_i$  concentrations, whereas other strains are better competitors at high  $\text{C}_i$  levels, causing a succession of different  $\text{C}_i$  uptake genotypes during bloom development. Models and laboratory experiments predict that rising atmospheric  $\text{CO}_2$  levels will lead to higher  $\text{CO}_2(\text{aq})$  and bicarbonate concentrations, and a later onset and shorter duration of  $\text{CO}_2$ -depleted conditions during dense summer blooms (14, 15). Our results suggest that this increased  $\text{C}_i$  availability will favor low-affinity but high-flux bicarbonate uptake genotypes. Hence, future harmful

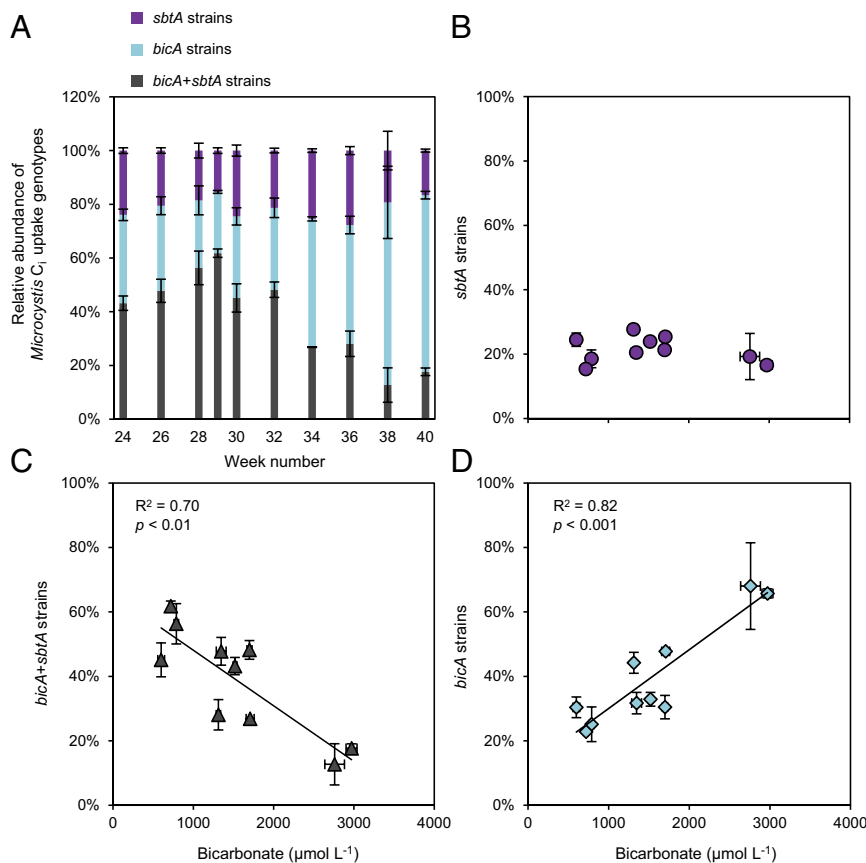


**Fig. 4.**  $C_i$  uptake genotypes of *Microcystis* in the lake study. (A) Relative abundances of the three  $C_i$  uptake genotypes (*sbtA* strains, *bicA* strains, and *bicA* + *sbtA* strains). (B–D) Relation between the relative abundances of the  $C_i$  uptake genotypes and the bicarbonate concentration. The data points show the mean ( $\pm$ SD) of three replicate measurements. The trend lines are based on linear regression ( $n = 10$ ).

cyanobacterial blooms will most likely have a genotype composition that differs from contemporary blooms and will be adapted to the new conditions in a high- $CO_2$  world.

## Materials and Methods

**Competition Experiments.** Competition experiments were conducted in  $CO_2$ -controlled chemostats designed specifically for phytoplankton studies (14, 31, 49). The chemostats consisted of flat culture vessels with an optical path length of 5 cm and an effective working volume of 1.8 L. The chemostats were illuminated from one side at a constant incident irradiance of  $I_{in} = 40 \mu\text{mol photons}\cdot\text{m}^{-2}\cdot\text{s}^{-1}$  using white fluorescent tubes (Philips Master TL-D 90 De Luxe 18 W/965; Philips Lighting). The chemostats were maintained at a constant temperature of 25 °C, using a nutrient-rich mineral medium without (bi)carbonate salts, and aerated with small gas bubbles containing either 100 or 1,000 ppm  $CO_2$  at a flow rate of 30  $L\cdot h^{-1}$  (31). The chemostats were run at a dilution rate of 0.2  $d^{-1}$ .

*Microcystis* strains CCAP 1450/10, HUB 5-2-4, PCC 7806, PCC 7005, and PCC 7941 (SI Appendix, Table S1) were precultured in monoculture chemostats at 400 ppm  $CO_2$ . Subsequently, six chemostats were each inoculated with the five precultured strains mixed at equal initial abundances and a total initial *Microcystis* biovolume of  $\sim 160 \text{ mm}^3\cdot L^{-1}$ . Three chemostats were exposed to 100 ppm  $pCO_2$  (“low  $CO_2$ ”) and the three other chemostats to 1,000 ppm  $pCO_2$  (“high  $CO_2$ ”). The chemostats were run for a total of 175 d and were sampled one to three times per week for further analysis. Cell numbers, biovolumes, light conditions, and pH were measured as described before (31).

**Lake Study.** Lake Kennemermeer (52°27′18.5″N, 4°33′48.6″E) is a shallow coastal dune lake located northwest of Amsterdam, The Netherlands, close to the North Sea (Fig. 2A). The lake is not an official swimming location, because of yearly recurrent problems caused by dense harmful cyanobacterial blooms. The lake has a maximum depth of  $\sim 1$  m and a surface area of  $\sim 0.1 \text{ km}^2$ . The lake is well mixed by wind throughout the year.

From June to October 2013, we sampled the lake two to three times per month, always at 10:30 AM, at a fixed location at the north side using a small

boat. Aliquots of lake water (three replicates of 5 L each) were collected 0.2 m below the surface and processed immediately on land. A hydroLab surveyor and Datasonde 4a (OTT Hydromet) measured temperature and pH at 0.2-m depth. Phytoplankton cells were preserved with Lugol’s iodine for microscopic analysis (SI Appendix, SI Materials and Methods).

**Chemical Analyses.** Dissolved inorganic carbon (DIC) and sodium concentrations were measured in filtered supernatant of the chemostat and lake samples.  $CO_2$ (aq), bicarbonate, and carbonate concentrations were calculated from DIC, pH, and temperature (SI Appendix, Table S5). Microcystins were extracted from filtered cells with 75% MeOH and analyzed by HPLC (49). See SI Appendix, SI Materials and Methods for details.

**Analysis of Genotype Composition.** Genomic DNA (gDNA) was isolated from chemostat samples and lake samples that were filtered on-site, using spin column DNA extraction kits (SI Appendix, SI Materials and Methods).

We first investigated whether all three *Microcystis*  $C_i$  uptake genotypes were present in purified gDNA lake samples, using PCR reactions with the GoTaq Hot Start Polymerase kit (Promega) according to the supplier’s instructions (SI Appendix, SI Materials and Methods). The *Microcystis*-specific primers used for this purpose are listed in SI Appendix, Table S3.

Subsequently, qPCR reactions were applied to purified gDNA to quantify the relative abundances of the different genotypes in the chemostat and lake samples (SI Appendix, SI Materials and Methods). For this purpose, we designed gene-specific primers to target the 16S rRNA gene, *rbcX*, *bicA*, *sbtA*, *bicA* + *sbtA*, *mcyB*, and *isiA* (SI Appendix, Table S3), using gDNA from axenic laboratory strains as reference samples. LinRegPCR software (v2012.3) was used for baseline correction, calculation of  $C_q$  values, and calculation of the amplification efficiency of individual runs (SI Appendix, Table S3). Relative ratios of the numbers of gene copies were calculated according to the comparative  $C_T$  method (50). The qPCR analysis was validated using defined mixtures of isolated *Microcystis* strains (SI Appendix, Fig. S4). Because our field data set was limited to one lake sampled during one summer, we did not

attempt to separate the statistical effects of many environmental variables on the genotype assemblage. Instead, we applied simple correlation analyses to describe relationships between the relative frequencies of the  $C_i$  uptake genotypes and the  $C_i$  concentration. The rate of replacement was estimated from the slope of the linear regression of  $\ln(x_1/x_2)$  versus time (51, 52), where  $x_1$  and  $x_2$  are the relative frequencies of two genotypes. The selection coefficient was calculated by scaling the replacement rate to the generation time (51). The generation time in the chemostats was calculated as  $t_d = \ln(2)/\mu$ , where  $\mu$  is the growth rate of the total *Microcystis* population (taking into account the dilution rate).

- Solomon S, et al., eds (2007) Climate change 2007: The physical science basis. *Contribution of Working Group I to the Fourth Assessment Report of the Intergovernmental Panel on Climate Change* (Cambridge Univ Press, Cambridge, UK).
- Meinshausen M, et al. (2011) The RCP greenhouse gas concentrations and their extensions from 1765 to 2300. *Clim Change* 109(1–2):213–241.
- Raven JA, Giordano M, Beardall J, Maberly SC (2012) Algal evolution in relation to atmospheric CO<sub>2</sub>: Carboxylases, carbon-concentrating mechanisms and carbon oxidation cycles. *Philos Trans R Soc Lond B Biol Sci* 367(1588):493–507.
- Collins S, Bell G (2004) Phenotypic consequences of 1,000 generations of selection at elevated CO<sub>2</sub> in a green alga. *Nature* 431(7008):566–569.
- Collins S, Sültemeyer D, Bell G (2006) Changes in C uptake in populations of *Chlamydomonas reinhardtii* selected at high CO<sub>2</sub>. *Plant Cell Environ* 29(9):1812–1819.
- Lohbeck KT, Riebesell U, Reusch TBH (2012) Adaptive evolution of a key phytoplankton species to ocean acidification. *Nat Geosci* 5(5):346–351.
- Low-Décarie E, Jewell MD, Fussmann GF, Bell G (2013) Long-term culture at elevated atmospheric CO<sub>2</sub> fails to evoke specific adaptation in seven freshwater phytoplankton species. *Philos Trans R Soc Lond B Biol Sci* 280(1754):20122598.
- Hutchins DA, et al. (2015) Irreversibly increased nitrogen fixation in *Trichodesmium* experimentally adapted to elevated carbon dioxide. *Nat Commun* 6:8155.
- Scheinin M, Riebesell U, Rynearson TA, Lohbeck KT, Collins S (2015) Experimental evolution gone wild. *J R Soc Interface* 12(106):20150056.
- Paerl HW, Huisman J (2008) Blooms like it hot. *Science* 320(5872):57–58.
- Qin B, et al. (2010) A drinking water crisis in Lake Taihu, China: Linkage to climatic variability and lake management. *Environ Manage* 45(1):105–112.
- Michalak AM, et al. (2013) Record-setting algal bloom in Lake Erie caused by agricultural and meteorological trends consistent with expected future conditions. *Proc Natl Acad Sci USA* 110(16):6448–6452.
- O’Neil JM, Davis TW, Burford MA, Gobler CJ (2012) The rise of harmful cyanobacteria blooms: The potential roles of eutrophication and climate change. *Harmful Algae* 14: 313–334.
- Verspagen JMH, et al. (2014) Rising CO<sub>2</sub> levels will intensify phytoplankton blooms in eutrophic and hypertrophic lakes. *PLoS One* 9(8):e104325.
- Visser PM, et al. (2016) How rising CO<sub>2</sub> and global warming may stimulate harmful cyanobacterial blooms. *Harmful Algae* 54:145–159.
- Ibelings BW, Maberly SC (1998) Photoinhibition and the availability of inorganic carbon restrict photosynthesis by surface blooms of cyanobacteria. *Limnol Oceanogr* 43(3):408–419.
- Balmer MB, Downing JA (2011) Carbon dioxide concentrations in eutrophic lakes: Undersaturation implies atmospheric uptake. *Inland Waters* 1(2):125–132.
- Gu B, Schelske CL, Coveney MF (2011) Low carbon dioxide partial pressure in a productive subtropical lake. *Aquat Sci* 73(3):317–330.
- Shapiro J (1997) The role of carbon dioxide in the initiation and maintenance of blue-green dominance in lakes. *Freshw Biol* 37(2):307–323.
- Low-Décarie E, Fussmann GF, Bell G (2011) The effect of elevated CO<sub>2</sub> on growth and competition in experimental phytoplankton communities. *Glob Change Biol* 17(8): 2525–2535.
- Price GD (2011) Inorganic carbon transporters of the cyanobacterial CO<sub>2</sub> concentrating mechanism. *Photosynth Res* 109(1–3):47–57.
- Rae BD, Förster B, Badger MR, Price GD (2011) The CO<sub>2</sub>-concentrating mechanism of *Synechococcus* WH5701 is composed of native and horizontally-acquired components. *Photosynth Res* 109(1–3):59–72.
- Sandrini G, Matthijs HCP, Verspagen JMH, Muyzer G, Huisman J (2014) Genetic diversity of inorganic carbon uptake systems causes variation in CO<sub>2</sub> response of the cyanobacterium *Microcystis*. *ISME J* 8(3):589–600.
- Price GD, Woodger FJ, Badger MR, Howitt SM, Tucker L (2004) Identification of a SulP-type bicarbonate transporter in marine cyanobacteria. *Proc Natl Acad Sci USA* 101(52): 18228–18233.
- Codd GA, Morrison LF, Metcalf JS (2005) Cyanobacterial toxins: Risk management for health protection. *Toxicol Appl Pharmacol* 203(3):264–272.
- Ibelings BW, Backer LC, Kardinaal WEA, Chorus I (2015) Current approaches to cyanotoxin risk assessment and risk management around the globe. *Harmful Algae* 49:63–74.
- Du J, Förster B, Rourke L, Howitt SM, Price GD (2014) Characterisation of cyanobacterial bicarbonate transporters in *E. coli* shows that SbtA homologs are functional in this heterologous expression system. *PLoS One* 9(12):e115905.
- Wilson AE, Sarnelle O, Tillmanns AR (2006) Effects of cyanobacterial toxicity and morphology on the population growth of freshwater zooplankton: Meta-analyses of laboratory experiments. *Limnol Oceanogr* 51(4):1915–1924.
- Tchernov D, et al. (2001) Passive entry of CO<sub>2</sub> and its energy-dependent intracellular conversion to HCO<sub>3</sub><sup>-</sup> in cyanobacteria are driven by a photosystem I-generated  $\Delta\mu\text{H}^+$ . *J Biol Chem* 276(26):23450–23455.
- Maeda S, Badger MR, Price GD (2002) Novel gene products associated with NdhD3/D4-containing NDH-1 complexes are involved in photosynthetic CO<sub>2</sub> hydration in the cyanobacterium, *Synechococcus* sp. PCC7942. *Mol Microbiol* 43(2):425–435.
- Sandrini G, Cunsolo S, Schuurmans JM, Matthijs HCP, Huisman J (2015) Changes in gene expression, cell physiology and toxicity of the harmful cyanobacterium *Microcystis aeruginosa* at elevated CO<sub>2</sub>. *Front Microbiol* 6:401.
- Sandrini G, Jakupovic D, Matthijs HCP, Huisman J (2015) Strains of the harmful cyanobacterium *Microcystis aeruginosa* differ in gene expression and activity of inorganic carbon uptake systems at elevated CO<sub>2</sub> levels. *Appl Environ Microbiol* 81(22):7730–7739.
- Sandrini G, et al. (2016) Diel variation in gene expression of the CO<sub>2</sub>-concentrating mechanism during a harmful cyanobacterial bloom. *Front Microbiol* 7:551.
- Sültemeyer D, Price GD, Yu JW, Badger MR (1995) Characterisation of carbon dioxide and bicarbonate transport during steady-state photosynthesis in the marine cyanobacterium *Synechococcus* strain PCC7002. *Planta* 197:597–607.
- Benschop JJ, Badger MR, Dean Price G (2003) Characterisation of CO<sub>2</sub> and HCO<sub>3</sub><sup>-</sup> uptake in the cyanobacterium *Synechocystis* sp. PCC6803. *Photosynth Res* 77(2–3): 117–126.
- Eichner M, Thoms S, Kranz SA, Rost B (2015) Cellular inorganic carbon fluxes in *Trichodesmium*: A combined approach using measurements and modelling. *J Exp Bot* 66(3):749–759.
- Visser PM, Passarge J, Mur LR (1997) Modelling vertical migration of the cyanobacterium *Microcystis*. *Hydrobiologia* 349(1):99–109.
- Verspagen JMH, et al. (2004) Recruitment of benthic *Microcystis* (Cyanophyceae) to the water column: Internal buoyancy changes or resuspension? *J Phycol* 40(2):260–270.
- Humbert JF, et al. (2013) A tribute to disorder in the genome of the bloom-forming freshwater cyanobacterium *Microcystis aeruginosa*. *PLoS One* 8(8):e70747.
- Harke MJ, et al. (2016) A review of the global ecology, genomics, and biogeography of the toxic cyanobacterium, *Microcystis* spp. *Harmful Algae* 54:4–20.
- Zilliges Y, et al. (2011) The cyanobacterial hepatotoxin microcystin binds to proteins and increases the fitness of *microcystis* under oxidative stress conditions. *PLoS One* 6(3):e17615.
- Geerts AN, et al. (2015) Rapid evolution of thermal tolerance in the water flea *Daphnia*. *Nat Clim Chang* 5(7):665–668.
- Padfield D, Yvon-Durocher G, Buckling A, Jennings S, Yvon-Durocher G (2015) Rapid evolution of metabolic traits explains thermal adaptation in phytoplankton. *Ecol Lett* 19(2):133–142.
- Yoshida T, Jones LE, Ellner SP, Fussmann GF, Hairston NG, Jr (2003) Rapid evolution drives ecological dynamics in a predator-prey system. *Nature* 424(6946):303–306.
- Meyer JR, Ellner SP, Hairston NG, Jr, Jones LE, Yoshida T (2006) Prey evolution on the time scale of predator-prey dynamics revealed by allele-specific quantitative PCR. *Proc Natl Acad Sci USA* 103(28):10690–10695.
- Hairston NG, Ellner SP, Geber MA, Yoshida T, Fox JA (2005) Rapid evolution and the convergence of ecological and evolutionary time. *Ecol Lett* 8(10):1114–1127.
- Buckling A, Craig Maclean R, Brockhurst MA, Colegrave N (2009) The Beagle in a bottle. *Nature* 457(7231):824–829.
- Schoener TW (2011) The newest synthesis: Understanding the interplay of evolutionary and ecological dynamics. *Science* 331(6016):426–429.
- Van de Waal DB, et al. (2011) Reversal in competitive dominance of a toxic versus non-toxic cyanobacterium in response to rising CO<sub>2</sub>. *ISME J* 5(9):1438–1450.
- Livak KJ, Schmittgen TD (2001) Analysis of relative gene expression data using real-time quantitative PCR and the 2<sup>- $\Delta\Delta\text{CT}$</sup>  method. *Methods* 25(4):402–408.
- Dykhuizen DE, Hartl DL (1983) Selection in chemostats. *Microbiol Rev* 47(2):150–168.
- Passarge J, Hol S, Escher M, Huisman J (2006) Competition for nutrients and light: Stable coexistence, alternative stable states, or competitive exclusion? *Ecol Monogr* 76(1):57–72.